 CMES, vol.11, no.1, pp.27-36, 2006

Passive Electric Potential CT Method Using Piezoelectric Material for Identification of Plural Cracks

Daiki Shiozawa[1], **Shiro Kubo**[2], **Takahide Sakagami**[2] **and Masaaki Takagi**[2]

Abstract: The passive electric potential CT (computed tomography) method using piezoelectric film was applied to the identification of plural through cracks. The use of piezoelectric material made it possible to obtain electric potential field without applying electric current. For identification of cracks an inverse analysis scheme based on the least residual method was applied, in which square sum of residuals is evaluated between the measured electric potential distributions and those computed by using the finite element method. The Akaike information criterion (AIC) was used to estimate the number of cracks. Numerical simulations were carried out on the identification of plural cracks and a single crack. The location and size of these cracks were quantitatively estimated by the present method. The number of cracks was correctly estimated, even when the plural cracks were closely located and the measured electric potential distribution was similar to that for a single crack.

keyword: Nondestructive evaluation, Crack identification, Electric potential CT method, Passive nondestructive method, Piezoelectric film, Damage monitoring , Plural cracks, Inverse analysis, Akaike information criterion

1 Introduction

Non-destructive and real-time damage monitoring technique is important for maintenance of structures, such as power plants, chemical plants, aircrafts, space structures and bridges. Non-destructive crack identification is recognized as a domain/boundary inverse problem (see Kubo 1988), which deals with the estimation of an unknown boundary. Conventional NDT (non-destructive testing) methods, such as ultrasonic method, radiation method, electric potential method may not be applied for the purpose, since they have some limitations in their applications for automatic inspection, non-contact inspection or remote inspection in severe environment. The intelligent structures (see Crawley 1987) provide us continuous and real-time signals concerning damage initiation and propagation, and then have a function of self-damage detection and monitoring and contribute to prevention of catastrophic failure of the structure. With the use of estimated crack size, shape and location, evaluation of facture mechanics parameters can be made (see for example, So et al. 2004, Guo and Naim 2004, Chen and Chen 2005, Sladek et al. 2005)

Piezoelectric film is a sensing device that generates an electrical charge proportional to a change in mechanical strain. Several investigations have been conducted on the development of intelligent structures using piezoelectric materials. Galea et al. (1993) showed the possibility of the use of piezoelectric PVDF (poly vinylidene fluoride) film as a sensing device for detecting and monitoring damages in composite materials. Yin et al. (1995) carried out numerical analyses to demonstrate the feasibility of applying PVDF film for damage detection in composites. Li and some of the present authors (2000) made theoretical and numerical investigation on the development of crack identification technique for the structures on which piezoelectric material was installed.

Some of the present authors (Kubo et al. 1986, 1991, Sakagami et al. 1988) proposed the active electric potential CT (computed tomography) method for quantitative identification of two- and three-dimensional cracks, by applying inverse analyses to electric potential distributions observed under electric current application. The passive electric potential CT method, which did not require the application of electric current, was also proposed by gluing piezoelectric film on a cracked body subjected to mechanical load (Shiozawa et al. 2002). In this method the quantitative crack identification was made from the distribution of electric potential observed on the surface of piezoelectric film. Numerical simulations and

[1] Department of Mechanical Engineering, Kobe University, 1-1, Rokkodai, Nada, Kobe 657-8501, Japan
[2] Department of Mechanical Engineering, Graduate School of Engineering, Osaka University, 2-1, Yamadaoka, Suita, Osaka, 565-0871, Japan

experiments showed the applicability of the method to the identification of a single crack (Shiozawa et al. 2002, 2004a, 2004b).

In this paper, the applicability of the method to the identification of plural cracks is examined. The effects of the distance between cracks, crack location and crack size on the electric potential distribution are investigated by the finite element analyses. Numerical simulations are carried out on the estimation of location, size and the number of plural through cracks, based on the inverse analyses.

2 Analysis of Electric Potential Distributions

2.1 Method of Analysis

When piezoelectric film is glued on the surface of cracked plate subjected to mechanical load, a change in electric potential distribution is observed on the surface of piezoelectric film. The FEM (finite element method) computer analysis scheme was developed for coupled elastic and electric potential problem to investigate the relationship between crack parameters and electric potential distribution on the piezoelectric film. The governing equations of the coupled strain field and electric filed of piezoelectric material can be written as (see IEEE 1978);

$$\{\boldsymbol{\sigma}\} = [\mathbf{C}]\{\boldsymbol{\varepsilon}\} - [\mathbf{e}]^T\{\mathbf{E}\} \tag{1}$$

$$\{\mathbf{D}\} = [\mathbf{e}]\{\boldsymbol{\varepsilon}\} + [\mathbf{g}]\{\mathbf{E}\} \tag{2}$$

where $\{\boldsymbol{\sigma}\}$ and $\{\boldsymbol{\varepsilon}\}$ are stress and strain vectors, $[\mathbf{C}]$, $[\mathbf{e}]$ and $[\mathbf{g}]$ are stiffness matrix, piezoelectric coefficient matrix and dielectric constant matrix, respectively. $\{\mathbf{E}\}$ is electric field vector. $\{\mathbf{D}\}$ is electric displacement vector. The static FEM equations, based on Eqs. (1) and (2), are obtained as,

$$\begin{aligned} &[\boldsymbol{K}_{uu}]\{\mathbf{d}\} + [\boldsymbol{K}_{u\phi}]\{\boldsymbol{\phi}\} = \{\mathbf{F}\} \\ &[\boldsymbol{K}_{u\phi}]\{\mathbf{d}\} + [\boldsymbol{K}_{\phi\phi}]\{\boldsymbol{\phi}\} = \{\mathbf{Q}\} \end{aligned} \tag{3}$$

where $[\boldsymbol{K}_{uu}]$, $[\boldsymbol{K}_{u\phi}]$ and $[\boldsymbol{K}_{\phi\phi}]$ are the mass matrix, displacement electric stiffness matrix and electric stiffness matrix, respectively. $\{\boldsymbol{d}\}$, $\{\boldsymbol{\phi}\}$, $\{\boldsymbol{F}\}$ and $\{\boldsymbol{Q}\}$ are the displacement vector, the electric potential vector, the mechanical load vector and the electric load vector, respectively.

From Eq. (3), coupled property between an elastic field and an electric potential field is given in $[\boldsymbol{K}_{u\phi}]$.

The present method can be applied to structures or components subjected to mechanical load, which gives rise to electric potential change on the piezoelectric film. A simple model containing plural through cracks subjected to uniform tension shown in Fig. 1 is employed for simulations. This model consists of an elastic substrate material made of A2024 aluminum alloy and a piezoelectric film. PVDF (poly vinylidene fluoride) film was used as the piezoelectric film.

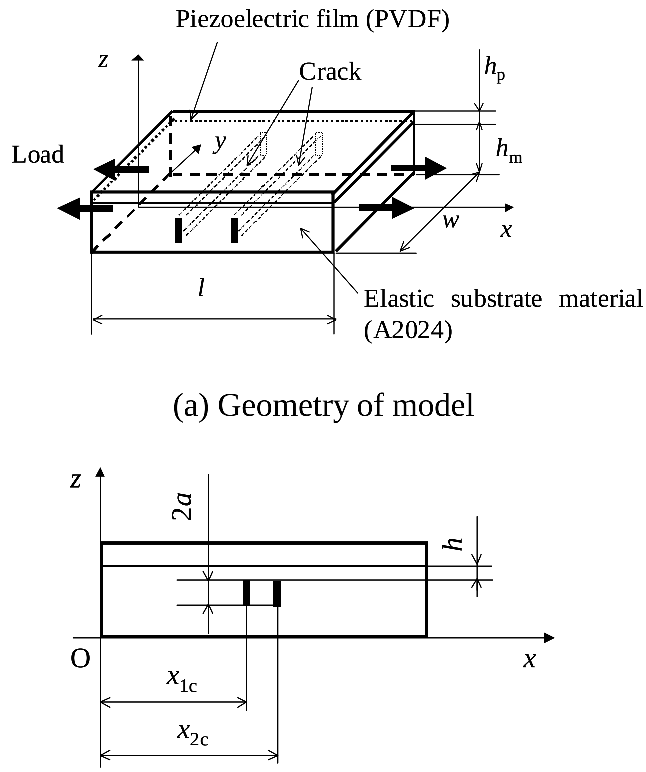

(a) Geometry of model

(b) Crack parameters

Figure 1 : Model of plural cracks used in analyses (dimensions in mm)

Crack parameters are chosen as follows: a is half length of the crack, h is crack depth from top surface of the plate, and x_{1c} and x_{2c} designate crack location of the cracks in the x-direction. For simplicity the lengths, and also the depths, of the plural cracks are assumed to be equal. The properties of the piezoelectric material are shown in Table 1 (Tashiro et al. 1981). Young's modulus E_m, shear modulus G_m, Poisson's ratio ν_m and density ρ_m of A2024 aluminum alloy used as a substrate material are shown in Table 2. It was assumed that the potential

Table 1 : Properties of the piezoelectric film

Elastic properties ($\times 10^9$N/m^2)	c_{11}	3.61
	c_{12}	1.61
	c_{13}	1.42
	c_{33}	1.60
	c_{44}	0.550
Piezoelectric properties ($\times 10^{-3}$C/m^2)	e_{31}	42.0
	e_{33}	-6.0
	e_{15}	-59.0
Dielectric properties ($\times 10^{-12}$C/Vm)	g_{11}	106.3
	g_{33}	106.3
Density (10^3kg/m^3)	ρ	1.75
Thickness (mm)	t_{piezo}	0.04

Table 2 : Properties of the elastic substrate material (A2024 aluminum alloy)

E_m	G_m	ν_m	ρ_m
72.4 (GPa)	27.1 (GPa)	0.33	2.77 (10^3kg/m^3)

on the interface between the elastic material and PVDF film is 0. The load was set to be 1960 (N).

2.2 Electric Potential Distributions

Effects of crack length a and crack depth h on the electric potential distribution in the case that the plate has only one crack are shown in Figs. 2 and 3, respectively (Shiozawa et al. 2004a). As is seen in the figures the distribution has two peaks taking a peak value of ϕ_{max}. The distribution is symmetrical with respect to the line of the crack, and therefore, the location of local minimum between the two peaks of potential coincides with the location of crack. The peak value of electric potential ϕ_{max} increases with increase in crack length a.

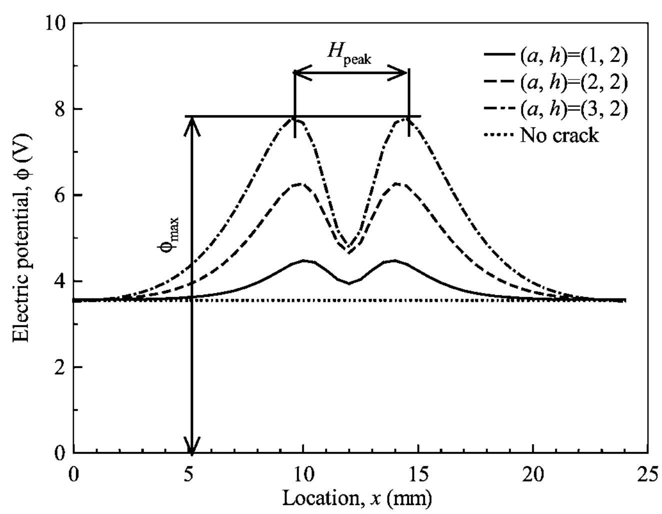

Figure 2 : Effect of crack length a on electric potential distributions for a plate with a single crack

When the plate has two cracks, the distance between the cracks (x_{2c}- x_{1c}) has significant effect on the distribution of electric potential distribution. Figure 4 examines the effect of the distance between plural cracks keeping the length a and depth h constant. When the cracks are located apart, there are two peaks on the electric potential distribution near each of the cracks, and in total there are four peaks. When the cracks are located closer as in the case of x_{1c}=13 and x_{2c}=16 shown by a chained line in Fig. 4, the number of the peaks on the electric potential distributions is reduced to three. When the cracks are located much closer as in the cases of x_{1c}=14 and x_{2c}=16, or x_{1c}=15 and x_{2c}=16, the number of the peaks on the electric potential distributions is reduced to two and is similar to that for a single crack shown by a dotted line in the figure. Then it is not possible to judge whether the number of cracks is 1 or 2 from the number of the peaks on the electric potential distribution.

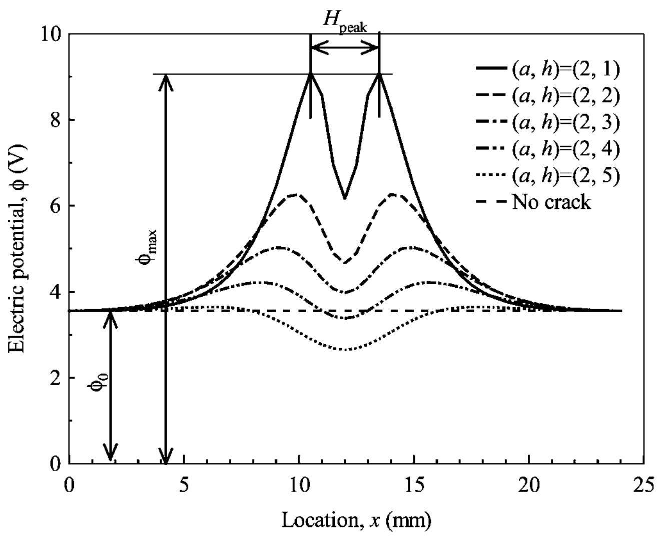

Figure 3 : Effect of crack depth h on electric potential distributions for a plate with a single crack

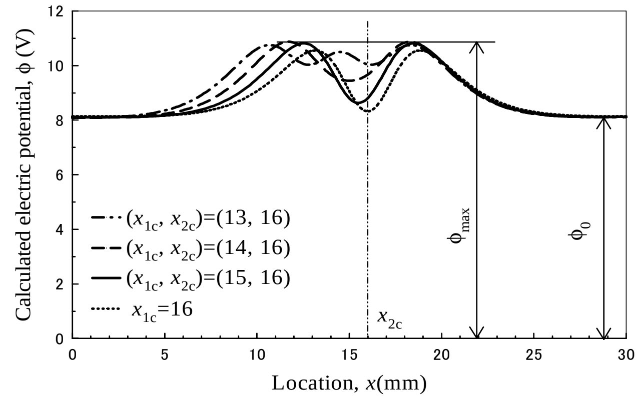

Figure 4 : Effect of distance between cracks $(x_{2c} - x_{1c})$ on electric potential distributions for a plate with plural cracks with length of a=2 and depth of h=3.

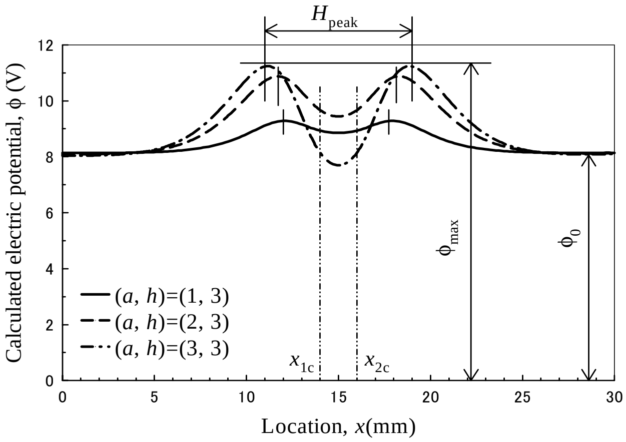

Figure 5 : Effect of crack length a on electric potential distributions for a plate having plural cracks with depth of h=3 located at x_{1c}=14 and x_{2c}=16.

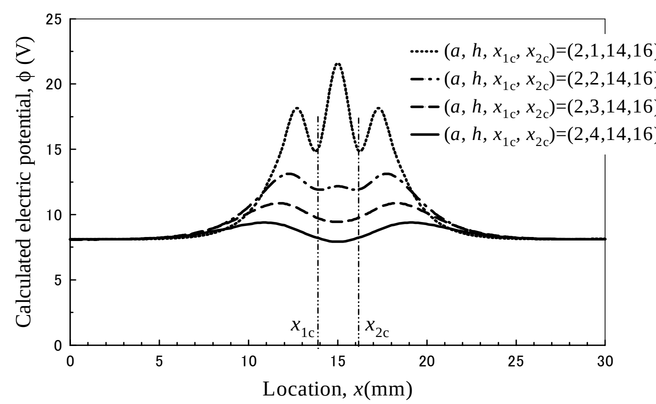

Figure 6 : Effect of crack depth h on electric potential distributions for a plate having plural cracks with length of a=2 located at x_{1c}=14 and x_{2c}=16.

Examples of effects of crack length a and crack depth h on the electric potential distribution for a plate with plural cracks are shown in Figs. 5 and 6, respectively. As is seen in the figures the peaks in the electric potential distributions are pronounced for large values of crack length a and for small values of crack depth h.

3 Inverse Analysis for Crack Identification

As the inverse analysis method for identification of cracks, the least residual method was applied (Kubo et al. 1986). In this method, computed values $\phi^{(c)}$ are compared with the measured valuesg$\phi^{(m)}$ to determine the most plausible crack location and size. As a criterion for crack identification the following square sum R_s of residuals is calculated.

$$R_s(a,h,x_{1c},x_{2c}) = \sum_i^M (\phi_i^{(c)}(a,h,x_{1c},x_{2c}) - \phi_i^{(m)})^2 \qquad (4)$$

Here $\phi_i^{(m)}$ denotes measured electric potential value at the i-th measuring point, and $\phi_i^{(c)}(a,\ h,\ x_{1c},\ x_{2c})$ denotes the electric potential values at the i-th measuring point computed by the FEM, in which crack parameters are assumed to be a, h, x_{1c} and x_{2c}. The values of a, h, x_{1c} and x_{2c} are denoted in mm. M is the total number of measuring points. The combination of crack location and size,

Table 3 : Parameters of cracks used in the numerical simulations of crack identification

		Crack parameters			
		A	h	x_{1c}	x_{2c}
Plural cracks	Crack 1	2.4	3.9	11.3	27.4
	Crack 2	2.4	3.9	13.2	17.7
	Crack 3	2.4	3.9	13.7	16.6
Single crack	Crack 4	2.4	3.9	16.2	—

which minimized R_s, was employed as the most plausible one among all the assumed combinations of the crack location and size.

For effective inverse analysis, the following hierarchical calculation steps were introduced.

In the first step, crack parameters are roughly estimated. The crack location in the x-direction x_{jc} (j=1, ..., n_c) is determined from the location of local minimum between two peaks in the electric potential distribution. Here n_c denotes the number of cracks. In the estimation of a and h, $R_s$is calculated for the combinations of three crack lengths and three crack depths. It is assumed that R_s is approximated by the following quadratic function of a and h.

$$R_s(a,h,x_{jc}) = A + Ba + Cah + Da^2 + Eh + Fh^2 \tag{5}$$

Coefficients A, B, C, D, E and F are determined by the least-squares method from the values of R_s for the combinations of three crack lengths and three crack depths. The combination of a and h, which minimized this approximate function for R_s, is employed as the plausible combination in the rough estimation of crack parameters.

In the second step, the combination of crack parameters, which gives the minimum R_s, is searched by using the modified Powell optimization method (Zangwill 1964). The crack parameters obtained in the above rough estimation are used as the initial values of the crack parameters for the modified Powell method.

To estimate the number of cracks the Akaike information criterion (AIC) (Akaike 1978) was used (Kubo et al. 1997). AIC is a measure for evaluating the fitness of the model based on the Bayes procedure. AIC is defined by the following equation for the present problem.

$$AIC = N\ log_e(R_s/N) + 2P \tag{6}$$

Here N denotes the total number of measurements and P is the number of crack parameters. The number of cracks giving the smallest value of AIC is taken as the plausible one.

4 Numerical Simulation of Crack Identification

4.1 *Cracks and Electric Potential Distributions Used in the Simulations*

Numerical simulations are made for three types of plural cracks and a single crack, whose crack parameters are shown in Table 3. Three types of plural cracks, i.e. Cracks 1, 2 and 3 are used. To examine the applicability of the AIC to the estimation of the number of cracks a single crack, Crack 4, is also included in the crack models of simulations. To simulate the experimental acquisition of potential $\phi_i^{(m)}$, artificial noise was added to the computed values obtained by the FEM. As the noise levels, 0.5%, 1.0% and 3.0% were selected. Artificial noise was introduced using a uniform random number. On the surface of PVDF film, electric potential was measured at points placed with an interval of 0.5 (mm). The total number of measurements N is equal to 61 for Cracks 2, 3 and 4, and is 81 for Crack 1.

The electric potential distributions for Crack 1 through 4 are shown in Fig. 7. For Crack 1 the distance between the plural cracks are so large that there are 4 peaks in the electric potential distributions. For Crack 2 the distance is smaller and the number of the peaks is reduced to 3 due to the interference of peaks of electric potential distributions. For Crack 3 the distance is further smaller and there are only 2 peaks in the electric potential distribution as for Crack 4, which is a single crack.

4.2 *Results of Identification*

The crack parameters were estimated using the least residual method with the modified Powell method assuming that the cracks were single or plural. The number of

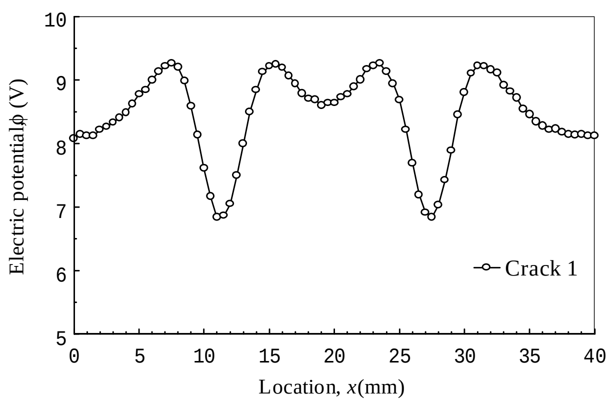

(a) Crack 1

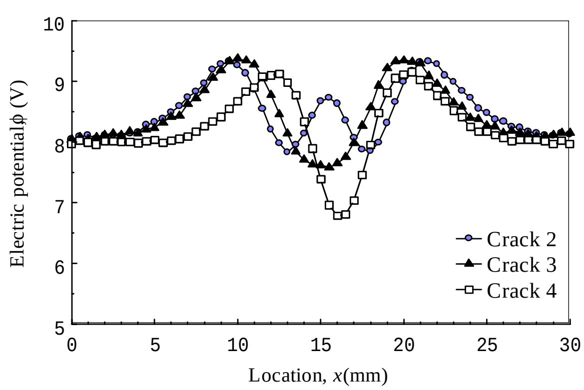

(a) Cracks 2, 3 and 4

Figure 7 : Electric potential distributions for cracks 1, 2, 3 and 4.

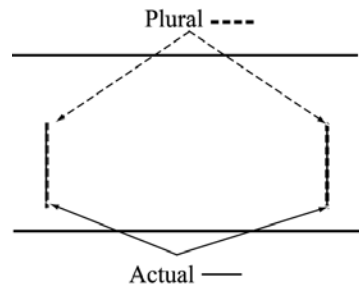

Figure 8 : Geometries of estimated and actual cracks in the identification of Crack 1

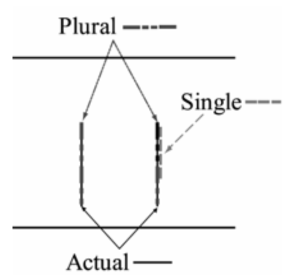

Figure 9 : Geometries of estimated and actual cracks in the identification of Crack 2

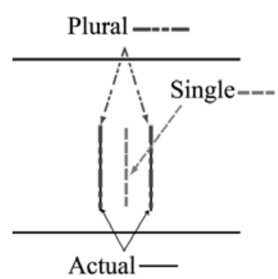

Figure 10 : Geometries of estimated and actual cracks in the identification of Crack 3

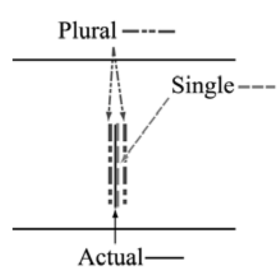

Figure 11 : Geometries of estimated and actual cracks in the identification of Crack 4

cracks was estimated using AIC. The results of rough estimate of crack parameters when the cracks are assumed to be single and plural are shown for Cracks 1, 2, 3 and 4 in Tables 4, 5, 6 and 7, respectively. The results of detailed estimated of crack parameters when the cracks are assumed to be single and plural are shown with the values of residual R_s and AIC for Cracks 1, 2, 3 and 4 in Tables 8, 9, 10 and 11, respectively. The geometries of estimated cracks and actual ones are shown in Figs. 8 through 11. In these figures actual cracks are shown by solid lines. Estimated cracks assuming a single and plural cracks are shown by dashed lines and chained lines, respectively.

By comparing Tables 4 through 7 with Tables 8 through 11, it is seen that the estimation of the crack parameters is made effectively by applying the hierarchical scheme. For plural cracks, i.e. Cracks 1, 2 and 3, the value of AIC

Table 4 : Rough estimate of crack parameters from the electric potential distributions in the identification of Crack 1

Crack type	Noise level	Crack parameters			
		a	h	x_{1c}	x_{2c}
	Actual	2.4	3.9	11.3	27.4
Plural cracks	0.5 %	1.469	2.995	11.0	27.5
	1.0 %	1.470	2.995	11.0	27.5
	3.0 %	1.465	2.987	11.0	27.5

Table 5 : Rough estimate of crack parameters from the electric potential distributions in the identification of Crack 2

Crack type	Noise level	Crack parameters			
		a	h	x_{1c}	x_{2c}
	Actual	2.4	3.9	13.2	17.7
Single cracks	0.5 %	1.472	3.537	15.5	-
	1.0 %	1.472	3.537	15.5	-
	3.0 %	1.469	3.540	15.5	-
Plural cracks	0.5 %	1.503	3.047	13.0	18.0
	1.0 %	1.503	3.603	13.0	18.0
	3.0 %	1.506	3.601	13.0	18.0

Table 6 : Rough estimate of crack parameters from the electric potential distributions in the identification of Crack 3

Crack type	Noise level	Crack parameters			
		a	h	x_{1c}	x_{2c}
	Actual	2.4	3.9	13.7	16.6
Single cracks	0.5 %	1.493	3.574	15.5	-
	1.0 %	1.492	3.573	15.5	-
	3.0 %	1.495	3.570	15.5	-
Plural cracks	0.5 %	1.523	3.073	14.0	17.0
	1.0 %	1.498	3.589	14.0	17.0
	3.0 %	1.495	3.592	14.0	17.0

Table 7 : Rough estimate of crack parameters from the electric potential distributions in the identification of Crack 4

Crack type	Noise level	Crack parameters			
		a	h	x_{1c}	x_{2c}
	Actual	2.4	3.9	16.2	-
Single cracks	0.5 %	1.462	3.526	16.0	-
	1.0 %	1.462	3.526	16.0	-
	3.0 %	1.465	3.526	16.0	-
Plural cracks	0.5 %	1.484	3.586	15.0	17.0
	1.0 %	1.484	3.586	15.0	17.0
	3.0 %	1.484	3.586	15.0	17.0

Table 8 : Detailed estimate of crack parameters from the electric potential distributions in the identification of Crack 1

Crack type	Noise level	Crack parameters				R_s
		a	h	x_{1c}	x_{2c}	
	Actual	2.4	3.9	11.3	27.4	
Plural cracks	0.5 %	2.389	3.905	11.26	27.39	0.0721
	1.0 %	2.391	3.898	11.28	27.38	0.1606
	3.0 %	2.432	3.849	11.30	27.40	1.841

Table 9 : Detailed estimate of crack parameters from the electric potential distributions in the identification of Crack 2

Crack type	Noise level	Crack parameters				R_s	AIC
		a	h	x_{1c}	x_{2c}		
	Actual	2.4	3.9	13.2	17.7		
Single crack	0.5 %	1.511	4.122	17.87		10.88	99
	1.0 %	1.522	4.141	17.78		11.12	98
	3.0 %	1.407	3.971	18.00		11.67	95
Plural cracks	0.5 %	2.400	3.902	13.18	17.71	0.037	444
	1.0 %	2.408	3.893	13.19	17.68	0.175	349
	3.0 %	2.390	3.893	13.23	17.71	1.269	228

Table 10 : Detailed estimate of crack parameters from the electric potential distributions in the identification of Crack 3

Crack type	Noise level	Crack parameters				R_s	AIC
		a	h	x_{1c}	x_{2c}		
	Actual	2.4	3.9	13.7	16.6		
Single crack	0.5 %	2.180	4.030	15.18		3.362	171
	1.0 %	2.190	4.030	15.16		3.536	168
	3.0 %	2.215	4.043	15.11		3.493	147
Plural cracks	0.5 %	2.396	3.902	13.69	16.59	0.039	440
	1.0 %	2.404	3.895	13.71	16.61	0.174	350
	3.0 %	2.430	3.890	13.66	16.59	1.470	219

Table 11 : Detailed estimate of crack parameters from the electric potential distributions in the identification of Crack 4

Crack type	Noise level	Crack parameters				R_s	AIC
		a	h	x_{1c}	x_{2c}		
	Actual	2.4	3.9	16.2			
Single crack	0.5 %	2.403	3.901	16.19		0.041	440
	1.0 %	2.405	3.899	16.20		0.134	367
	3.0 %	2.412	3.890	16.30		1.524	219
Plural cracks	0.5 %	2.380	3.940	15.86	16.52	0.060	415
	1.0 %	2.378	3.940	15.81	16.56	0.169	351
	3.0 %	2.382	3.931	15.87	16.74	1.529	217

assuming the cracks are plural is smaller than that assuming the cracks are single, indicating that the estimated number of cracks is 2. This is the case even for Crack 3, for which the number of peaks in the electric potential distributions is 2 as in the case of a single crack. For Crack 4, which is the single crack, the values of residual R_s assuming a single crack and plural cracks are close, especially when the noise level is high. The value of AIC assuming the cracks are plural is larger than that assuming that the cracks are single, indicating that the estimated number of cracks is 1. Thus the number of the cracks is correctly estimated based on AIC.

It is seen from these tables and figures that the crack parameters are estimated with good accuracies, even when the noise level is 3%. Experimental investigations (Shiozawa et al. 2002) showed that the noise level was around several percent when a non-contact type measurement system was applied.

In our related papers the passive electric potential CT method was applied to the identification of three-dimensional surface crack (Shiozawa et al. 2002b) and to the identification of delamination in CFRP composites (Shiozawa et al. 2003, Nakatani et al. 2005), and the usefulness of the method was shown.

5 Conclusions

The passive electric potential CT method using piezoelectric film was applied to the identification of plural through cracks. In this method cracks are identified based on the inverse analysis using the least residual method from the electric potential distribution observed on piezoelectric PVDF film glued on cracked plate subjected to mechanical load. The number of cracks was estimated using the Akaike information criterion (AIC). Numerical simulations of identification of plural cracks and a single crack were carried out. Crack parameters were estimated with good accuracies up to the noise level of 3% in the observed electric potential distribution. The number of cracks was correctly estimated, even when the cracks were closely located and the number of peaks in the electric potential distribution was the same with that for a single crack.

Acknowledgement: This work is partly supported by the Japan Society of Promotion of Science under the Grant-in-Aid for Scientific Research.

References

Akaike, H. (1978): A New Look ay the Bayes Procedure. *Biometrica,* vol. **65**, pp. 53-59.

Chen, Wen-Hwa; Chen, Cheng-Hung (2005): On Three-Dimensional Fracture Mechanics Analysis by an Enriched Meshless Method. *CMES: Computer Modeling in Engineering and Sciences,* vol. **8**, pp. 177-190.

Crawley, E. F.; Luist, J. (1987): Use of Piezoelctric Actuator as Elements of Intelligent Structures. *AIAA Journal*, vol. **25**, pp. 1375-1385.

Gelea, S. C.; Chiu, W. K.; Paul, J. J. (1993): Use of Piezoelectric Films in Detecting and Monitoring Damage in Composites. *International Journal of Intelligent Material Systems and Structures*, vol. **4**, pp. 330-336.

IEEE (1978): IEEE Standard on Piezoelectricity. *IEEE/ANSI Std.*

Guo, Y.; Nairn, J. A. (2004): Calculation of J-Integral and Stress Intensity Factors using the Material Point Method. *CMES: Computer Modeling in Engineering and Sciences,* vol. **6**, pp. 295-308.

Kubo, S. (1988): Inverse Problems Related to the Mechanics and Fracture of Solids and Structures. JSME *International Journal, Series I*, The Japan Society of Mechanical Engineers, vol. **31**, pp. 157-166

Kubo, S.; Sakagami, T.; Ohji, K. (1986): Electric Potential CT Method Based on BEM Inverse Analyses for Measurement of Three-Dimensional Cracks. In: G. Yagawa and S.N. Atluri (ed) *Computational Mechanics '86,* Vol. 1, Springer, pp. V-339-V-344.

Kubo, S.; Sakagami, T.; Ohji, K. (1991): The Electric Potential CT Method for Measuring Two- and Three-Dimensional Cracks. In: H. Okamura and K. Ogura (ed) *Current Japanese Materials Research- Vol.8 Fracture Mechanics,* Elsevier Applied Science, The Society of Materials Science, Japan, pp. 235-254.

Kubo, S.; Ohji, K.; Aoe, S. (1997): Identification of Plural Cracks by the Electric Potential CT Method Using Fusion-Type Genetic Algorithm. *Proc. of Int. Conf. on Advanced Technology in Experimental Mechanics*, The Japan Society of Mechanical Engineers, pp. 105-110.

Li, S.-Q.; Kubo, S.; Sakagami, T.; Liu, Z.-X. (2000): Theoretical and Numerical Investigation on Crack Identification Using Piezoelectric Material-Embedded Structures. *Material Science Research International.*, The Society of Materials Science, Japan, vol. **6**, pp. 41-48.

Nakatani, N.; Kubo, S.; Sakagami, S.; Shiozawa, S.; Takagi, M. (2005): An Experimental Study on Identification of Delamination in Composite Material by the Passive Electric Potential CT Method. In D. Lesnic (ed): *Proc. 5th Int. Conf. on Inverse Problems in Engineering*, Leeds University Press, vol. III, pp. N02.1-N02.10.

Sakagami, T.; Kubo, S.; Hashimoto, T.; Yamawaki, H.; Ohji, K. (1988): Quantitative Measurement of Two-Dimensional Inclined Cracks by the Electric-Potential CT Method with Multiple Current Applications. *JSME Int. J., Series I*, The Japan Society of Mechanical Engineers, vol. **31**, pp.76-86.

Shiozawa, D.; Kubo, S.; Sakagami, T.; Okuno, K. (2002): An Experimental Study on Applicability of Passive Electric Potential CT Method to Crack Identification. *Journal of the Society of Material Science, Japan*, vol. **51**, pp. 926-931.

Shiozawa, D.; Kubo, S.; Sakagami, T. (2003): Identification of Delamination Defect in Laminated Composites by Passive Electric Potential CT Method. In: M. Tanaka and G.S. Dulikravich (ed) *Inverse Problems in Engineering Mechanics IV,* Elsevier, pp.195-203.

Shiozawa, D.; Kubo, S.; Sakagami, T. (2004a): Passive Electric Potential CT Method Using Piezoelectric Material for Crack Identification. *Inverse Problems in Science and Engineering*, vol. **12**, pp.71-79

Shiozawa, D.; Kubo, S.; Sakagami, T. (2004b): An Experimental Study on Applicability of Passive Electric Potential CT Method to Crack Identification. *JSME International Journal, Series* A, The Japan Society of Mechanical Engineers, vol. **47**, pp. 419-425.

Shiozawa, D.; Kubo, S.; Sakagami, T.; Okazaki, S. (2005): An Experimental Study on Applicability of Passive Electric Potential CT Method to Identification of Three-Dimensional Crack. *Trans. of the Japan Society of Mechanical Engineers*, vol.11, pp. 1038-1045.

Sladek, J.; Sladek, V.; Krivacek, J.; Zhang, Ch. (2005): Meshless Local Petrov-Galerkin Method for Stress and Crack Analysis in 3-D Axisymmetric FGM Bodies. *CMES: Computer Modeling in Engineering and Sciences,* vol. **8**, pp. 259-270.

So, W.M.G.; Lau, K.J.; Ng, S.W. (2004): Determination of Stress Intensity Factors for Interfacial Cracks Using the Virtual Crack Extension Approach. *CMES: Computer Modeling in Engineering and Sciences,* vol. **5**, pp. 189-200.

Tashiro, T.; Tadokoro, H.; Kobayashi, M. (1981): Structure and Piezoelectricity of Poly(Vinylidene Fluoride). *Ferroelectrics*, vol. **32**, pp. 167-175.

Yin, L.; Wang, X.-M.; Shen, Y.-P. (1995): Damage-Monitoring in Composite Laminates by Piezoelectric Films. *Computers and Structures*, vol. **59**, pp. 623-630.

Zangwill, W. I. (1964): Minimizing a Function without Calculating Derivatives. *Computer Journal.*, vol. **7**, pp. 149-154.